HHS Public Access

Author manuscript

Bone. Author manuscript; available in PMC 2018 June 04.

Published in final edited form as:

Bone. 2017 April ; 97: 209–215. doi:10.1016/j.bone.2017.01.032.

Administration of an activin receptor IIB ligand trap protects male juvenile rhesus macaques from simian immunodeficiency virus-associated bone loss

Wen Guo[a,*], **Karol M Pencina**[a], **Karyn O'Connell**[b], **Monty Montano**[a], **Liming Peng**[a], **Susan Westmoreland**[b], **Julie Glowacki**[c], and **Shalender Bhasin**[a]

[a]Research Program in Men's Health: Aging and Metabolism, Brigham and Women's Hospital, Harvard Medical School, Boston, MA 02115, United States

[b]Department of Comparative Pathology, New England Primate Research Center, One Pine Hill Drive, PO Box 9102, Southborough, MA 01772-9102, United States

[c]Department of Orthopedic Surgery, Brigham and Women's Hospital, Harvard Medical School, Boston, MA 02115, United States

Abstract

HIV-infected individuals are at an increased risk of osteoporosis despite effective viral suppression. Observations that myostatin null mice have increased bone mass led us to hypothesize that simian immunodeficiency virus (SIV)-associated bone loss may be attenuated by blocking myostatin/TGFβ signaling. In this proof-of-concept study, pair-housed juvenile male rhesus macaques were inoculated with SIVmac239. Four weeks later, animals were treated with vehicle or Fc-conjugated soluble activin receptor IIB (ActR2B·Fc, iv. 10 mg $*$ kg^{-1} $*$ $week^{-1}$) – an antagonist of myostatin and related members of TGFβ superfamily. Limb and trunk bone mineral content (BMC) and density (BMD) using dual-energy X-Ray absorptiometry, circulating markers of bone growth and turnover, and serum testosterone levels were measured at baseline and during the 12-week intervention period. The increase in BMC was significantly greater in the ActRIIB.Fc-treated group (+8 g) than in the placebo group (−4 g) ($p < 0.05$). BMD also increased significantly more in the ActRIIB.Fc-treated macaques (+0.03 g/cm^2) than in the placebo-treated animals (+0 g/cm^2) ($p < 0.005$). Serum osteocalcin was about two-fold higher in the ActRIIB.Fc-treated group than in the placebo group ($p < 0.05$), but serum C-terminal telopeptide and testosterone levels did not differ significantly between groups. The expression levels of TNFalpha ($p < 0.05$), GADD45 ($p <b 0.005$), and sclerostin ($p < 0.038$) in the bone-marrow were significantly lower in the ActRIIB.Fc-treated group than in the placebo group.

Conclusion—The administration of ActRIIB.FC in SIV-infected juvenile macaques significantly increases BMC and BMD in association with reduced expression levels of markers of bone marrow inflammation.

*Corresponding author. wguo2@partners.org.

Supplementary data to this article can be found online at http://dx.doi.org/10.1016/j.bone.2017.01.032.

Disclosure statement

The authors have nothing to disclose.

Keywords

Nonhuman primate; Bone; Soluble activin receptor IIB; SIV

1. Introduction

Although antiretroviral therapy has profoundly reduced morbidity and mortality associated with human immunodeficiency virus (HIV) infection, the loss of bone mass remains a significant concern even among HIV-infected individuals on highly active anti-retroviral therapy [1–5]. The past decade has witnessed considerable investment in the development of novel pharmacologic therapies for the treatment of musculoskeletal decline associated with HIV and other chronic diseases. Among the novel pharmacologic therapies in development are function-promoting drugs such as myostatin antagonists and selective androgen receptor modulators. Myostatin is a highly conserved member of the TGFβ superfamily and is expressed in adult skeletal muscle as well as in the adipose tissue and the cardiac muscle [6–8]. Spontaneous mutations in myostatin gene are associated with muscle hyperplasia and hypertrophy in a number of mammalian and non-mammalian species [9–12]. Conversely, over-expression of myostatin is associated with loss of muscle mass [13–15].

Several strategies to inhibit myostatin action have been tested for their ability to increase muscle mass in postnatal life in preclinical models and in a limited number of human trials [16–18]. These studies have revealed new roles for myostatin in other physiological systems, including the bone. Myostatin null mice exhibit increased bone strength and bone mineral density in limbs, trunk, and jaw compared to wild type mice [19–23]. Like other members of TGFβ superfamily, myostatin activates signaling upon binding to a heterodimeric complex made up of type 2 receptors activin receptor 2B/2A and type 1 receptors activin receptor-like kinase 4/5 (Alk4/5) [24]. Activin receptor IIB is expressed on the surface of many cell types including osteoblasts [25]. In a recent single ascending-dose study, ActRIIB.Fc increased serum bone-specific alkaline phosphatase and decreased serum C-terminal type I collagen telopeptide levels in healthy post-menopausal women [26]. ActRIIB.Fc increases bone mass in both limbs and vertebrae [27] and prevents bone loss caused by androgen deprivation in mice [28]. The bone anabolic effect of ActRIIB.Fc is observed even in myostatin null mice [27], suggesting the involvement of additional TGFβ/BMP ligands [29–31].

Chronic HIV infection has been associated with osteoporosis and an increased risk for fractures [32–34]. Furthermore, increased myostatin expression has been shown in HIV-infected patients with wasting [35]. Juvenile macaques experience a failure to thrive and bone loss when inoculated with SIV in a manner similar to that observed in HIV-infected children [36]. Accordingly, we conducted a proof-of-concept placebo-controlled trial in a nonhuman primate model of SIV-infection to test the hypothesis that administration of an ActRIIB.Fc ligand trap would attenuate the loss of bone mass associated with SIV-infection. The SIV model closely parallels the human disease and, therefore, was utilized to study the effects of ActRIIB.Fc on bone mineral content, bone mineral density, and bone markers.

2. Methods

Male rhesus macaques were pair-housed in a centralized Animal Biosafety Level 2 (ABSL-2) facility at the New England Primate Research Center and were maintained in accordance with the Guide for the Care and Use of Laboratory Animals (ILAR, 8th edition, 2011). The study protocol was approved by Harvard Medical School's Standing Committee on Animals. Macaques were fed a certified commercial primate diet (8714; Teklad) and provided fresh water *ad libitum*.

2.1. Animal assignment

Fourteen male juvenile (2.5–3-year-old) rhesus macaques (*Macaca mulatta*) were studied. All macaques were inoculated intravenously with SIVmac239 (50 ng of p27 viral-antigen equivalent) and randomized into two groups with seven animals per group based on age and major histocompatibility complex status. Four weeks after SIV inoculation, the treated group was injected from weeks 4 to 16 with ActRIIB.Fc (10 mg/kg/week, intramuscular), an experimental grade biologic provided by Dr. Carl Morris (Pfizer, Inc., Cambridge, MA, USA). The animals in the control group received weekly injections of an equal volume of a saline placebo.

The details of the baseline characteristics and longitudinal health status during the intervention period have been published [37]. One animal in the treated group was euthanized due to early AIDS-like symptoms. Among the 13 animals that completed the study, two were excluded because of unusually higher levels of serum testosterone than the other animals, likely caused by the earlier than expected onset of puberty. Another animal in the control group was excluded as it showed large gains in body mass and bone mass during the experimental period (above 3 times interquartile range outlier limit calculated for the rest of the sample), whereas all other animals in its group lost body mass or bone mass, as expected [38].

Dual energy X-ray absorptiometry (*DXA) scans* were performed with a total body scanner (Lunar, GE Healthcare, Westborough, MA, USA), by generating x-rays at 2 energy levels (40 and 70 kVp) as previously described [38]. Animals were sedated with Ketamine HCl (10 mg/kg) intramuscularly. A series of transverse scans were obtained from head to toe, at 1-cm intervals. Data were collected for ~120 pixel elements/transverse scan, with a pixel size of 5 × 10 mm. Bone mineral density (BMD) and bone mineral content (BMC) were derived using the computer algorithms provided by the manufacturer. As the juvenile macaques included in the study were still growing, bone mineral content was used as the primary outcome.

2.2. RT-qPCR

Bone marrow was harvested from the femur bone at the time of necropsy and stored frozen at −80°C. Tissue samples were homogenized in 3 volumes of Trizol (#15596018, Invitrogen, Carlsbad, CA, USA) on ice. RNA was purified using RNeasy mini kit (#74134, Qiagen, Valencia, CA, USA). Single strand cDNA was synthesized using ProtoScript® First Strand cDNA Synthesis Kit (#E6300S, New England Biolabs, Ipswich, MA, USA) following the

manufacturer's instruction. Real-time PCR was performed using SYBR master mix on an ABI 7500 Sequence Detection System (Thermo-Fisher, Waltham, MA, USA). Primer sequences are listed together with the corresponding gene bank accession number in Supplemental table 1 (Table S1).

2.3. Serum testosterone measurement

Serum testosterone was measured using liquid chromatography tandem mass spectrometry (LC-MS/MS). This assay has been certified by the Centers for Disease Control's Hormone Assay Standardization Program for Testosterone (HoST) and described previously [39]. The lower limit of quantification of the assay is 0.01 ng/mL. Inter-assay coefficients of variation were 7.8%, 5.9%, and 3.5%, at testosterone concentrations of 2.5, 5.0, and 10.0-ng/mL respectively.

2.4. Serum ELISA

Monkey C-telopeptide of type I collagen ELISA Kit (MBS737402) and Monkey N-terminal & mid-regional Osteocalcin ELISA Kit (MBS744305) were purchased from Mybiosource (www.mybiosource.com) and used following the manufacturer's instruction.

2.5. Statistical analyses

All statistical analyses were performed using SAS 9.3 software (SAS Institute, Cary NC) and Prism software (version 4.0c; GraphPad Software Inc.). For changes in BMC and BMD, between baseline and subsequent time points during intervention, a marginal model with repeated measures was performed to take into account within subject correlation. All models contained baseline covariate, treatment and time effects and were tested for significance of time and treatment interaction. If interaction was not significant, it was removed from the model and analyses focused on overall treatment effect. Pearson correlation coefficients with corresponding p-values were calculated for the relation of the change in BMC and BMD with the gene-expression levels as well as the change in lean body mass. For the comparisons of two independent samples, *t*-test and non-parametric Wilcoxon-Mann-Whitney tests were performed for normally distributed and non-normal data, respectively. Statistical significance in all tests was assigned at 0.05 level of alpha.

3. Results

3.1. ActRIIB.Fc administration increases bone mineral content and density

The rhesus macaques used in this studied were 2.5 to 3 years old, an age at which the macaques are undergoing pre-pubertal skeletal growth. Over the 16 week period, the body mass and lean mass remained unchanged in the control group, whereas a significant increase in lean mass was found in the ActRIIB.FC-treated group, as we recently reported [37]. Values of BMC and BMD were determined at baseline (4 weeks after SIV inoculation and right before treatment was initiated) and repeated during week 8 and week 16 after SIV inoculation (after 4 and 12 weeks of intervention). As shown in Fig. 1A, total body BMC declined with time in the control group while a reverse trend was detected in the ActRIIB.Fc-treated group. There was a significantly greater gain of BMC in animals assigned to the ActRIIB.Fc group than in those assigned to the control group ($p < 0.05$). In

addition, longitudinal measurements of the trunk and arms revealed greater gains in the regional BMC in the ActRIIB.Fc group than in the placebo group (Fig. 1C–D). Changes in the leg BMC followed the same trend although the difference did not reach statistical significance (Fig. 1E, $p = 0.165$). The BMD declined in the control group during the intervention group but increased significantly in ActRIIB.Fc-treated macaques (Fig. 1B). Overall, there was a significantly greater increase in BMD in the treatment group from week 4 to 16 than in the control group ($p < 0.05$). Detailed changes for individual animals are shown in supplemental Fig. S1.

3.2. The effects of ActRIIB.Fc on serum bone markers

Osteocalcin (OTC), the main non-collagenous hydroxyapatite-binding protein synthesized by osteoblasts, is a marker of osteoblast activity [40]. ActRIIB.Fc administration resulted in significantly higher serum OTC levels than saline administration (Fig. 2A, $p = 0.004$). Serum concentrations of CTX-I, a marker of bone resorption [40], did not differ between the groups (Fig. 2B), neither did serum concentrations of calcium and inorganic phosphate (not shown).

3.3. The effects of ActRIIB.Fc on serum testosterone level

SIV infection was associated with a progressive decline in serum testosterone levels in both groups with no significant difference between the two groups (Fig. 2C). At the end of the experiment, mRNA expression of androgen receptor in the femoral bone marrow also revealed no significant between the two groups (Fig. 2D).

3.4. The effects of ActRIIB.Fc on bone marrow gene expression

Analysis of bone marrow by RT-qPCR revealed lower expression levels of TNFα in the ActRIIB.FC-treated group than that in the control group (Fig. 3A), in line with prior reports that myostatin suppression leads to reduced serum TNFα level [41]. Bone marrow expression of GADD45, the gene for growth arrest and DNA damage repair and also a downstream target of TGFβ signaling [42], was lower in the ActRIIB.Fc-treated group as compared to the control group (Fig. 3B). The gains in BMC were negatively associated with GADD45 and TNFα (Fig. 3C–D) expression levels [43–48].

Sclerostin (SOST) is a newly established inhibitor of osteoblastic bone formation [43–45]. Although SOST is normally expressed in osteocytes, it can be induced in osteoblasts and osteoclasts by inflammatory bone diseases [46–49]. Consistent with the reduction in marrow TNFα expression, a significant reduction in SOST mRNA (Fig. 4A) coupled with a borderline significant reduction in plasma SOST level ($p = 0.07$, Fig. 4B) was found in the ActRIIB.Fc group.

We also examined bone marrow expression of a panel of genes related to bone formation and resorption, including markers of osteoblast and osteoclast activity (Fig. S2), the Wnt co-receptors and antagonists, as well as the RANKL to OPG ratio (Fig. S3). However, no significant between-group differences in the expression of these genes were detected.

3.5. Correlation between bone mass and body lean mass

Bone mass is positively correlated with skeletal muscle mass [50,51]. We found that the ActRIIB.Fc-associated gain in BMC was positively correlated with the gain in lean body mass (Fig. 5A, $r = 0.68$, $p = 0.03$). A borderline significant positive association was also observed between the changes in BMD and the gain in lean body mass (Fig. 5B, $r = 0.59$, $p = 0.07$).

The systemic viral burden, $CD4^+$ cell counts and the ratio of $CD4^+/CD8^+$ cell counts were not significantly different between the two groups (Fig. S4). Similarly, blood glucose (Fig. S5A) and serum cholesterol concentrations did not differ between groups (Fig. S5B).

4. Discussion

Our study provides the first evidence that administration of ActRIIB.Fc, a potent antagonist of myostatin and related ligands in the TGFβ superfamily, prevents the loss of bone mineral content and bone mineral density in SIV-infected juvenile macaques. This study provides the rationale for targeting activin receptor IIB ligands to prevent and reverse the HIV-associated loss of bone mass [37].

Administration of ActRIIB.FC was associated with significantly higher serum osteocalcin level, suggesting increased osteoblastic bone formation. This effect was associated with reduced bone marrow expression of TNFα, GADD45 and SOST in the SIV-infected monkeys. This observation is in agreement with previous reports that these genes are mutually inducible and subject to induction during chronic inflammatory diseases and by myostatin *per se* [41,47,52]. Importantly, treatment with ActRIIB.Fc results in continuous bone growth without affecting serum testosterone levels, suggesting that its bone effect occurs independently or downstream of testosterone, consistent with a previous report that ActRIIB.Fc reverses bone loss induced by androgen-deprivation in rodents [28]. It will be interesting to determine if co-administration of ActRIIB.Fc with testosterone may generate additive or synergistic anabolic effect, an approach that may also provide useful mechanistic insights for each drug.

The gains in BMC were positively associated with gains in lean body mass. We do not know whether the observed increases in BMC and BMD represent a direct effect of the ActRIIB.Fc on the bone or an indirect effect resulting from increased muscle mass. Positive correlation between muscle mass and bone mass has been reported with partial or complete myostatin inactivation in mice [50,51,53,54]. Recent studies suggest that myostatin may have direct catabolic effects on bone metabolism [55–58].

The pathophysiologic mechanisms of bone loss and bone growth arrest in HIV/SIV-infection are not completely understood. Circulating mediators of inflammation and immune activation, general catabolic effects of the virus, and suppression of sex hormones and growth factors are likely contributors. Our data indicate that changes in total BMC is associated with the increased expression levels of inflammatory marker TNFα and GADD45 in SIV-infected macaques. In addition, serum testosterone levels, which would have been expected to rise with age in the pre-pubertal juvenile macaques, were suppressed after SIV-

infection. The bone anabolic effect of testosterone has been well-documented in human and animals including boys reaching puberty [28,59–64], a developmental stage mirrored in our non-human primate model. Thus, our data suggest that low testosterone and inflammation, two consequences of SIV infection, may contribute to the bone growth arrest and loss of bone mass in placebo-treated, SIV-infected macaques.

While this manuscript was in preparation, a study of the effect of another ActRIIB.Fc molecule (ACE-031) in children with Duchenne muscular dystrophy (DMD) reported a trend towards increased bone mineral density [65]. This trial in children with DMD was stopped early because of increased frequency of nose and gum bleeding and telangiectasias in ActRIIB.Fc-treated subjects. We did not observe this adverse effect in our study using a different ActRIIB.Fc molecule. These differences in adverse effect profile between these compounds could reflect differences in the specificity of their binding to BMP9; it is also possible that the adverse effect noted in DMD patients could be due to an interaction of the molecule with the underlying disease because this adverse effect was not found in a prior study of the same molecule in postmenopausal women [26].

Limitations of this work include the small sample size of the study; the use of saline as placebo control rather than nonimmune serum; and the lack of a non-infected control group treated with placebo or active medication in parallel. Furthermore, the intervention duration of 12 weeks, although sufficient to demonstrate the hypothesized treatment effects on BMC and BMD, may not reflect bone effects under longer course treatment. Nevertheless, this study provides proof of concept of the potential therapeutic utility of ActRIIB.Fc treatment in prevention of bone loss in HIV infection, especially in the context of ART [66,67].

Supplementary Material

Refer to Web version on PubMed Central for supplementary material.

Acknowledgments

This work was supported in part by NIH grants DK078512, AG037193-06, AG037859, and P30AG031679. ActRIIB.Fc was generously provided by Dr. Carl Morris, Pfizer, Inc. Ron Desrosiers kindly supplied SIVmac239. Excellent animal care was provided by the veterinarians and veterinary technicians at NEPRC. SIV viral loads were analyzed by Jeff Lifson and Mike Piatak at NCI, AIDS and Cancer Virus Program. The necropsy service was provided by Elizabeth Curran at NEPRC.

Abbreviations

(SIV)	Simian immunodeficiency virus
(WPI)	weeks post-infection
(DXA)	dual energy X-ray absorptiometry
(AIDS)	acquired immunodeficiency syndrome
(HIV)	human immunodeficiency virus
(SAIDS)	Simian acquired immunodeficiency syndrome

References

1. Shikuma CM, Valcour VG, Ratto-Kim S, Williams AE, Souza S, Gerschenson M, Day L, Kim JH, Shiramizu B. HIV-associated wasting in the era of highly active anti-retroviral therapy-a syndrome of residual HIV infection in monocytes and macrophages. Clin Infect Dis. 2005; 40:1846–1848. [PubMed: 15909275]
2. Wanke CA, Silva M, Knox TA, Forrester J, Speigelman D, Gorbach SL. Weight loss and wasting remain common complications in individuals infected with human immunodeficiency virus in the era of highly active antiretroviral therapy. CID. 2000; 31:803–805.
3. Kusko RL, Banerjee C, Long KK, Darcy A, Otis J, Sebastiani P, Melov S, Tarnopolsky M, Bhasin S, Montano M. Premature expression of a muscle fibrosis axis in chronic HIV infection. Skelet Muscle. 2012; 2:10. [PubMed: 22676806]
4. Kooij KW, Wit FW, Bisschop PH, Schouten J, Stolte IG, Prins M, van der Valk M, Prins JM, van Eck-Smit BL, Lips P, Reiss P. Low bone mineral density in patients with well-suppressed HIV infection is largely explained by body weight, smoking and prior advanced HIV disease. J Infect Dis. 2014
5. Mora S, Puzzovio M, Giacomet V, Fabiano V, Maruca K, Capelli S, Nannini P, Lombardi G, Zuccotti GV. Sclerostin and DKK-1: two important regulators of bone metabolism in HIV-infected youths. Endocrine. 2015; 49:783–790. [PubMed: 25596857]
6. McPherron AC, Lawler AM, Lee SJ. Regulation of skeletal muscle mass in mice by a new TGF-beta superfamily member. Nature. 1997; 387(6628):83–90. [PubMed: 9139826]
7. McPherron AC, Lee SJ. Suppression of body fat accumulation in myostatin-deficient mice. J Clin Invest. 2002; 109(5):595–601. [PubMed: 11877467]
8. McPherron AC, Lee SJ. Double muscling in cattle due to mutations in the myostatin gene. Proc Natl Acad Sci U S A. 1997; 94(23):12457–12461. [PubMed: 9356471]
9. Elkina Y, von Haehling S, Anker SD, Springer J. The role of myostatin in muscle wasting: an overview. J Cachex Sarcopenia Muscle. 2011; 2:143–151.
10. Mosher DS, Quignon P, Bustamante CD, Sutter NB, Mellersh CS, Parker HG, Ostrander EA. A mutation in the myostatin gene increases muscle mass and enhances racing performance in heterozygote dogs. PLoS One. 2007; 3:79–86.
11. Chisada S, Okamoto H, Taniguchi Y, Kimori Y, Toyoda A, Sakaki Y, Takeda S, Yoshiura Y. Myostatin-deficient medaka exhibit a double-muscling phenotype with hyperplasia and hypertrophy, which occur sequentially during post-hatch development. Dev Biol. 2011; 359:82–94. [PubMed: 21925159]
12. Kambadur R, Sharma M, Smith TPL, Bass JJ. Mutations in myostatin (GDF8) in double-muscled Belgian Blue and Piedmontese cattle. Genome Res. 1997; 7:910–915. [PubMed: 9314496]
13. Zimmers TA, Davies MV, Koniaris LG, Haynes P, Esquela AF, Tomkinson KN, McPherron AC, Wolfman NM, Lee SJ. Induction of cachexia in mice by systemically administered myostatin. Science. 2002; 296:1486–1488. [PubMed: 12029139]
14. Durieux AC, Amirouche A, Banzet S, Koulmann N, Bonnefoy R, Pasdeloup M, Mouret C, Bigard X, Peinnequin A, Freyssenet D. Ectopic expression of myostatin induces atrophy of adult skeletal muscle by decreasing muscle gene expression. Endocrinology. 2007; 148:3140–3147. [PubMed: 17395701]
15. Elliott B, Renshaw D, Getting S, Mackenzie R. The central role of myostatin in skeletal muscle and whole body homeostasis. Acta Physiol (Oxford). 2012; 205:324–340.
16. Zhou X, Wang JL, Lu J, Song Y, Kwak KS, Jiao Q, Rosenfeld R, Chen Q, Boone T, Simonet WS, Lacey DL, Goldberg AL, Han HQ. Reversal of cancer cachexia and muscle wasting by ActRIIB antagonism leads to prolonged survival. Cell. 2010; 142:531–543. [PubMed: 20723755]
17. Liu W, Thomas SG, Asa SL, Gonzalez-Cadavid N, Bhasin S, Ezzat S. Myostatin is a skeletal muscle target of growth hormone anabolic action. J Clin Endocrinol Metab. 2003; 88:5490–5496. [PubMed: 14602795]
18. Wagner KR, Fleckenstein JL, Amato AA, Barohn RJ, Bushby K, Escolar DM, Flanigan KM, Pestronk A, Tawil R, Wolfe GI, Eagle M, Florence JM, King WM, Pandya S, Straub V, Juneau P, Meyers K, Csimma C, Araujo T, Allen R, Parsons SA, Wozney JM, Lavallie ER, Mendell JR. A

phase I/IItrial of MYO-029 in adult subjects with muscular dystrophy. Ann Neurol. 2008; 63:561–571. [PubMed: 18335515]

19. Hamrick MW. Increased bone mineral density in the femora of GDF8 knockout mice. Anat Rec A Discov Mol Cell Evol Biol. 2003; 272:388–391. [PubMed: 12704695]
20. Hamrick MW, McPherron AC, Lovejoy CO. Bone mineral content and density in the humerus of adult myostatin-deficient mice. Calcif Tissue Int. 2002; 71:63–68. [PubMed: 12060865]
21. Hamrick MW, McPherron AC, Lovejoy CO, Hudson J. Femoral morphology and cross-sectional geometry of adult myostatin-deficient mice. Bone. 2000; 27:343–349. [PubMed: 10962344]
22. Hamrick MW, Pennington C, Byron CD. Bone architecture and disc degeneration in the lumbar spine of mice lacking GDF-8 (myostatin). J Orthop Res. 2003; 21:1025–1032. [PubMed: 14554215]
23. Nicholson EK, Stock SR, Hamrick MW, Ravosa MJ. Biomineralization and adaptive plasticity of the temporomandibular joint in myostatin knockout mice. Arch Oral Biol. 2006; 51:37–49. [PubMed: 16054590]
24. Lee SJ, Reed LA, Davies MV, Girgenrath S, Goad ME, Tomkinson KN, Wright JF, Barker C, Ehrmantraut G, Holmstrom J, Trowell B, Gertz B, Jiang MS, Sebald SM, Matzuk M, Li E, Liang LF, Quattlebaum E, Stotish RL, Wolfman NM. Regulation of muscle growth by multiple ligands signaling through activin type II receptors. Proc Natl Acad Sci U S A. 2005; 102:18117–18122. [PubMed: 16330774]
25. Shuto T, Sarkar G, Bronk JT, Matsui N, Bolander ME. Osteoblasts express types I and II activin receptors during early intramembranous and endochondral bone formation. J Bone Miner Res. 1997; 12:403–411. [PubMed: 9076583]
26. Attie KM, Borgstein NG, Yang Y, Condon CH, Wilson DM, Pearsall AE, Kumar R, Willins DA, Seehra JS, Sherman ML. A single ascending-dose study of muscle regulator ACE-031 in healthy volunteers. Muscle Nerve. 2013; 47:416–423. [PubMed: 23169607]
27. Bialek P, Parkington J, Li X, Gavin D, Wallace C, Zhang J, Root A, Yan G, Warner L, Seeherman HJ, Yaworsky PJ. A myostatin and activin decoy receptor enhances bone formation in mice. Bone. 2014; 60:162–171. [PubMed: 24333131]
28. Koncarevic A, Cornwall-Brady M, Pullen A, Davies M, Sako D, Liu J, Kumar R, Tomkinson K, Baker T, Umiker B, Monnell T, Grinberg AV, Liharska K, Underwood KW, Ucran JA, Howard E, Barberio J, Spaits M, Pearsall S, Seehra J, Lachey J. A soluble activin receptor type IIb prevents the effects of androgen deprivation on body composition and bone health. Endocrinology. 2010; 151:4289–4300. [PubMed: 20573726]
29. Souza TA, Chen X, Guo Y, Sava P, Zhang J, Hill JJ, Yaworsky PJ, Qiu Y. Proteomic identification and functional validation of activins and bone morphogenetic protein 11 as candidate novel muscle mass regulators. Mol Endocrinol. 2008; 22:2689–2702. [PubMed: 18927237]
30. Townson SA, Martinez-Hackert E, Greppi C, Lowden P, Sako D, Liu J, Ucran JA, Liharska K, Underwood KW, Seehra J, Kumar R, Grinberg AV. Specificity and structure of a high affinity activin receptor-like kinase 1 (ALK1) signaling complex. J Biol Chem. 2012; 287:27313–27325. [PubMed: 22718755]
31. Sako D, Grinberg AV, Liu J, Davies MV, Castonguay R, Maniatis S, Andreucci AJ, Pobre EG, Tomkinson KN, Monnell TE, Ucran JA, Martinez-Hackert E, Pearsall RS, Underwood KW, Seehra J, Kumar R. Characterization of the ligand binding functionality of the extracellular domain of activin receptor type IIb. J Biol Chem. 2010; 285:21037–21048. [PubMed: 20385559]
32. Yong MK, Elliott JH, Woolley IJ, Hoy JF. Low CD4 count is associated with an increased risk of fragility fracture in HIV-infected patients. J Acquir Immune Defic Syndr. 2011; 57:205–210. [PubMed: 21522014]
33. Borderi M, Gibellini D, Vescini F, De Crignis E, Cimatti L, Biagetti C, Tampellini L, Re MC. Metabolic bone disease in HIV infection. AIDS. 2009; 23:1297–1310. [PubMed: 19550284]
34. Cazanave C, Dupon M, Lavignolle-Aurillac V, Barthe N, Lawson-Ayayi S, Mehsen N, Mercie P, Morlat P, Thiebaut R, Dabis F. Reduced bone mineral density in HIV-infected patients: prevalence and associated factors. AIDS. 2008; 22:395–402. [PubMed: 18195566]
35. Gonzalez-Cadavid NF, Taylor WE, Yarasheski K, Sinha-Hikim I, Ma K, Ezzat S, Shen R, Lalani R, Asa S, Mamita M, Nair G, Arver S, Bhasin S. Organization of the human myostatin gene and

expression in healthy men and HIV-infected men with muscle wasting. Proc Natl Acad Sci U S A. 1998; 95:14938–14943. [PubMed: 9843994]

36. Freeman LM, Mansfield KG, Lackner AA, Naumova EN, Gorbach SL. Survival and failure to thrive in the SIV-infected juvenile rhesus monkey. J Acquir Immune Defic Syndr. 1999; 22:119–123. [PubMed: 10843524]
37. O'Connell KE, Guo W, Serra C, Beck M, Wachtman L, Hoggatt A, Xia D, Pearson C, Knight H, O'Connell M, Miller AD, Westmoreland SV, Bhasin S. The effects of an ActRIIb receptor Fc fusion protein ligand trap in juvenile simian immunodeficiency virus-infected rhesus macaques. FASEB J. 2015; 29:1165–1175. [PubMed: 25466897]
38. Hendricks EE, Ludlage E, Bussell S, George K, Wegner FH, Mansfield KG. Wasting syndrome and disruption of the somatotropic axis in simian immunodeficiency virus-infected macaques with Mycobacterium avium complex infection. J Infect Dis. 2004; 190:2187–2194. [PubMed: 15551219]
39. Bhasin S, Zhang A, Coviello A, Jasuja R, Ulloor J, Singh R, Vesper H, Vasan RS. The impact of assay quality and reference ranges on clinical decision making in the diagnosis of androgen disorders. Steroids. 2008; 73:1311–1317. [PubMed: 18687348]
40. Lombardi G, Perego S, Luzi L, Banfi G. A Four-season Molecule: Osteocalcin, Updates in its physiological roles. Endocrine. 2014
41. Tang L, Yang X, Gao X, Du H, Han Y, Zhang D, Wang Z, Sun L. Inhibiting myostatin signaling prevents femoral trabecular bone loss and microarchitecture deterioration in diet-induced obese rats. Exp Biol Med (Maywood). 2015
42. Landesman Y, Bringold F, Milne DD, Meek DW. Modifications of p53 protein and accumulation of p21 and gadd45 mRNA in TGF-beta 1 growth inhibited cells. Cell Signal. 1997; 9:291–298. [PubMed: 9218130]
43. Baron R, Rawadi G. Wnt signaling and the regulation of bone mass. Curr Osteoporos Rep. 2007; 5:73–80. [PubMed: 17521509]
44. Baron R, Kneissel M. WNT signaling in bone homeostasis and disease: from human mutations to treatments. Nat Med. 2013; 19:179–192. [PubMed: 23389618]
45. Baron R, Saito H, Gori F. Bone cells crosstalk: noncanonical Roring in the Wnt. Cell Metab. 2012; 15:415–417. [PubMed: 22482722]
46. Vincent C, Findlay DM, Welldon KJ, Wijenayaka AR, Zheng TS, Haynes DR, Fazzalari NL, Evdokiou A, Atkins GJ. Pro-inflammatory cytokines TNF-related weak inducer of apoptosis (TWEAK) and TNFalpha induce the mitogen-activated protein ki-nase (MAPK)-dependent expression of sclerostin in human osteoblasts. J Bone Miner Res. 2009; 24:1434–1449. [PubMed: 19292615]
47. Almroth G, Lonn J, Uhlin F, Brudin L, Andersson B, Hahn-Zoric M. Sclerostin, TNF-alpha and interleukin-18 correlate and are together with Klotho related to other growth factors and cytokines in hemodialysis patients. Scand J Immunol. 2015
48. Baek K, Hwang HR, Park HJ, Kwon A, Qadir AS, Ko SH, Woo KM, Ryoo HM, Kim GS, Baek JH. TNF-alpha upregulates sclerostin expression in obese mice fed a high-fat diet. J Cell Physiol. 2014; 229:640–650. [PubMed: 24446199]
49. Kristensen IB, Christensen JH, Lyng MB, Moller MB, Pedersen L, Rasmussen LM, Ditzel HJ, Abildgaard N. Expression of osteoblast and osteoclast regulatory genes in the bone marrow microenvironment in multiple myeloma: only up-regulation of Wnt inhibitors SFRP3 and DKK1 is associated with lytic bone disease. Leuk Lymphoma. 2014; 55:911–919. [PubMed: 23915193]
50. Rauch F, Schoenau E. The developing bone: slave or master of its cells and molecules? Pediatr Res. 2001; 50:309–314. [PubMed: 11518815]
51. Frost HM. Muscle, bone, and the Utah paradigm: a 1999 overview. Med Sci Sports Exerc. 2000; 32:911–917. [PubMed: 10795780]
52. Invernizzi M, Carda S, Rizzi M, Grana E, Squarzanti DF, Cisari C, Molinari C, Reno F. Evaluation of serum myostatin and sclerostin levels in chronic spinal cord injured patients. Spinal Cord. 2015; 53:615–620. [PubMed: 25896346]
53. Chiu CS, Peekhaus N, Weber H, Adamski S, Murray EM, Zhang HZ, Zhao JZ, Ernst R, Lineberger J, Huang L, Hampton R, Arnold BA, Vitelli S, Hamuro L, Wang WR, Wei N, Dillon GM, Miao J,

Alves SE, Glantschnig H, Wang F, Wilkinson HA. Increased muscle force production and bone mineral density in ActRIIB-Fc-treated mature rodents. J Gerontol A Biol Sci Med Sci. 2013; 68:1181–1192. [PubMed: 23525481]

54. Oestreich AK, Carleton SM, Yao X, Gentry BA, Raw CE, Brown M, Pfeiffer FM, Wang Y, Phillips CL. Myostatin deficiency partially rescues the bone phenotype of osteogenesis imperfecta model mice. Osteoporos Int. 2015
55. Bowser M, Herberg S, Arounleut P, Shi X, Fulzele S, Hill WD, Isales CM, Hamrick MW. Effects of the activin A-myostatin-follistatin system on aging bone and muscle progenitor cells. Exp Gerontol. 2013; 48:290–297. [PubMed: 23178301]
56. Hamrick MW, Arounleut P, Kellum E, Cain M, Immel D, Liang LF. Recombinant myostatin (GDF-8) propeptide enhances the repair and regeneration of both muscle and bone in a model of deep penetrant musculoskeletal injury. J Trauma. 2010; 69:579–583. [PubMed: 20173658]
57. Dankbar B, Fennen M, Brunert D, Hayer S, Frank S, Wehmeyer C, Beckmann D, Paruzel P, Bertrand J, Redlich K, Koers-Wunrau C, Stratis A, Korb-Pap A, Pap T. Myostatin is a direct regulator of osteoclast differentiation and its inhibition reduces inflammatory joint destruction in mice. Nat Med. 2015; 21:1085–1090. [PubMed: 26236992]
58. Harslof T, Frost M, Nielsen TL, Husted LB, Nyegaard M, Brixen K, Borglum AD, Mosekilde L, Andersen M, Rejnmark L, Langdahl BL. Polymorphisms of muscle genes are associated with bone mass and incident osteoporotic fractures in Caucasians. Calcif Tissue Int. 2013; 92:467–476. [PubMed: 23370486]
59. James H 3rd, Aleksic I, Bienz MN, Pieczonka C, Iannotta P, Albala D, Mariados N, Mouraviev V, Saad F. Comparison of fracture risk assessment tool score to bone mineral density for estimating fracture risk in patients with advanced prostate cancer on androgen deprivation therapy. Urology. 2014; 84:164–168. [PubMed: 24976229]
60. Sinnesael M, Claessens F, Boonen S, Vanderschueren D. Novel insights in the regulation and mechanism of androgen action on bone. Curr Opin Endocrinol Diabetes Obes. 2013; 20:240–244. [PubMed: 23449008]
61. De Oliveira DH, Fighera TM, Bianchet LC, Kulak CA, Kulak J. Androgens and bone. Minerva Endocrinol. 2012; 37:305–314. [PubMed: 23235187]
62. Mantzoros CS, Flier JS, Rogol AD. A longitudinal assessment of hormonal and physical alterations during normal puberty in boys. V. Rising leptin levels may signal the onset of puberty. J Clin Endocrinol Metab. 1997; 82:1066–1070. [PubMed: 9100574]
63. Rochira V, Diazzi C, Santi D, Brigante G, Ansaloni A, Decaroli MC, De Vincentis S, Stentarelli C, Zona S, Guaraldi G. Low testosterone is associated with poor health status in men with human immunodeficiency virus infection: a retrospective study. Andrology. 2015; 3:298–308. [PubMed: 25704864]
64. Teichmann J, Lange U, Discher T, Lohmeyer J, Stracke H, Bretzel RG. Bone mineral density in human immunodeficiency virus-1 infected men with hypogonadism prior to highly-active-antiretroviral-therapy (HAART). Eur J Med Res. 2009; 14:59–64.
65. Campbell C, McMillan HJ, Mah JK, Tarnopolsky M, Selby K, McClure T, Wilson DM, Sherman ML, Escolar D, Attie KM. Myostatin inhibitor ACE-031 treatment of ambulatory boys with Duchenne muscular dystrophy: results of a randomized, placebo-controlled clinical trial. Muscle Nerve. 2016
66. McComsey GA, Tebas P, Shane E, Yin MT, Overton ET, Huang JS, Aldrovandi GM, Cardoso SW, Santana JL, Brown TT. Bone disease in HIV infection: a practical review and recommendations for HIV care providers. Clin Infect Dis. 2010; 51:937–946. [PubMed: 20839968]
67. Hansen AB, Obel N, Nielsen H, Pedersen C, Gerstoft J. Bone mineral density changes in protease inhibitor-sparing vs. nucleoside reverse transcriptase inhibitor-sparing highly active antiretroviral therapy: data from a randomized trial. HIV Med. 2011; 12:157–165. [PubMed: 20722752]

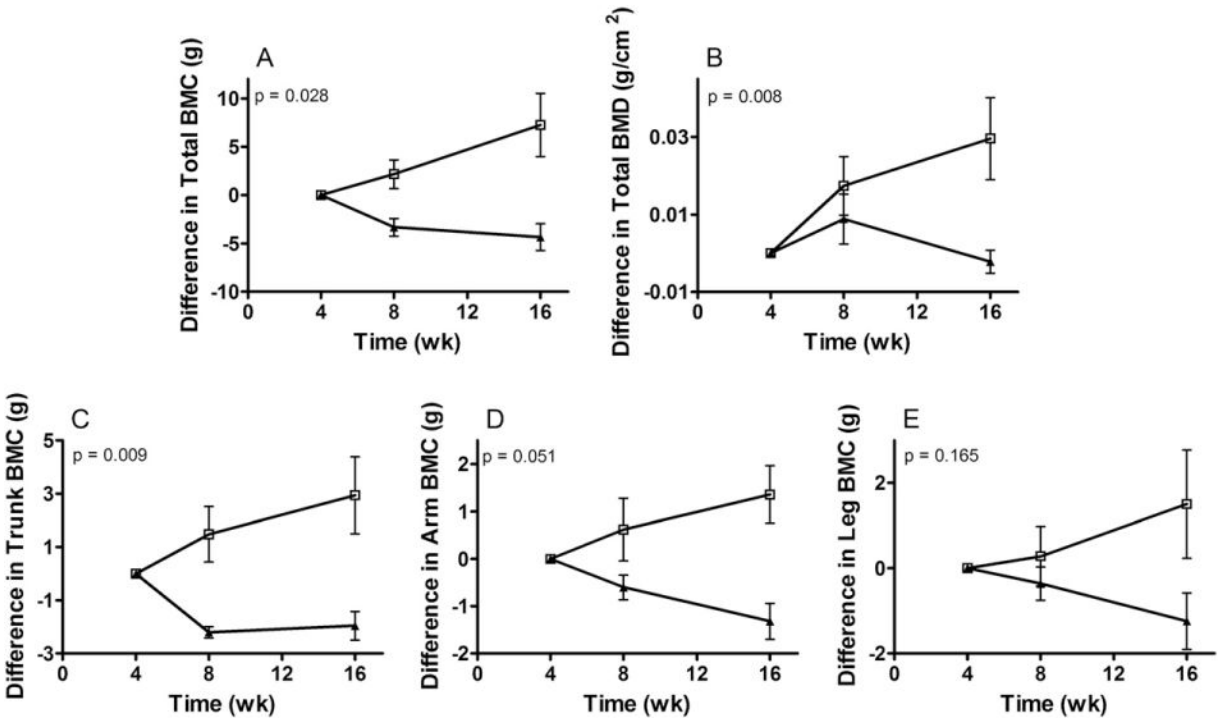

Fig. 1.

Effects of ActRIIB.Fc on SIV-induced bone loss. Rhesus monkeys were infected with SIV at time zero. Four weeks after the infection, half of the animals were randomly assigned to be treated with ActRIIB.Fc (□), and half with saline control (▲), by weekly injection. DEX scan was performed at wk. 4, 8, and 16. (A) Total BMC, (B) Total BMD, (C) Trunk BMC, (D) Arm BMC, (E) Leg BMC. Results are plotted as the difference between the measurement at each time point and that measured at wk. 4 (mean ± SE).

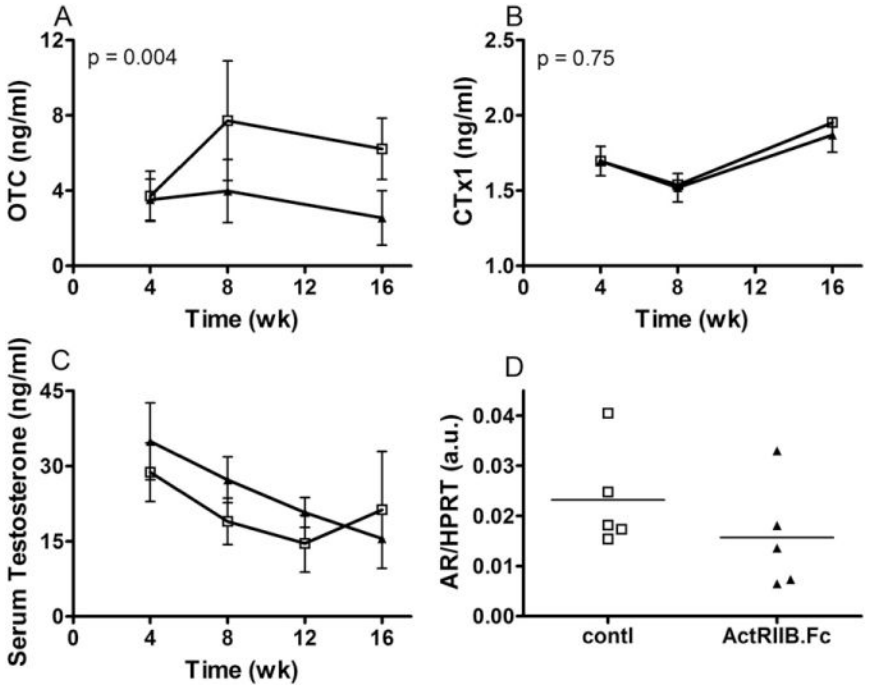

Fig. 2.

Effects of ActRIIB.Fc on serum osteocalcin (A: OTC), C-terminal telopeptide (B: CTx-1), Testosterone (C), and bone marrow expression of androgen receptor (D). Rhesus monkeys were infected with SIV once at zero time point, randomized four weeks later and treated with ActRIIB.Fc (□) and vehicle saline (▲), as described in Fig. 1. Serum levels of OTC and CTx-1 were analyzed by ELLISA. Serum testosterone was analyzed by LC-MS/MS. Results are plotted as mean ± 95%CI. Bone marrow mRNA in week 16 was analyzed by RT-qPCR, normalized to house-keeping gene HPRT, and analyzed by *t*-test. Each dot represents on individual animal.

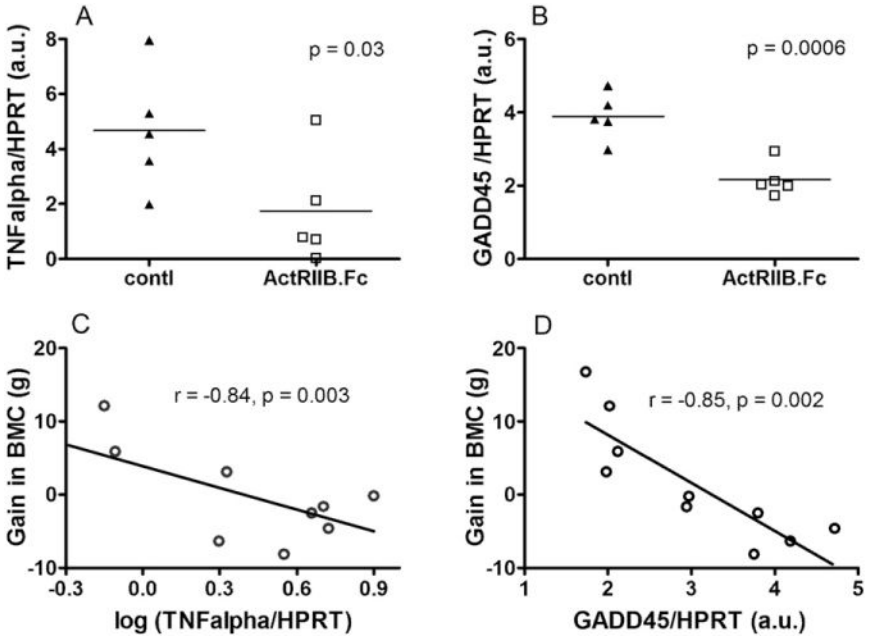

Fig. 3.

Effects of ActRIIB.Fc on bone marrow gene expression. Bone marrow was harvested at the end of treatment and analyzed by RT-qPCR for the expression of TNFα (A), and growth arrest and DNA damage gene 45 (B, GADD45), normalized to house-keeping gene HPRT (□, ActRIIB.Fc; ▲, saline control). Results were shown as dot plots with each dot represents on individual animal, and analyzed by unpaired *t*-test. Association between the gain in BMC and marrow gene expression for TNFα (C), and GADD45 (D), analyzed by Pearson correlation test.

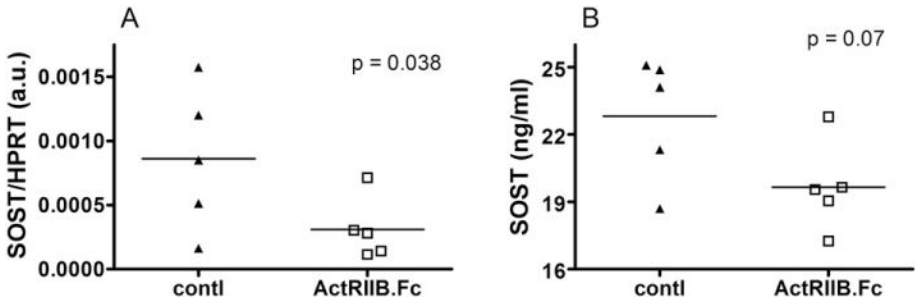

Fig. 4.

Effects of ActRIIB.Fc on sclerostin expression. (A) Bone marrow mRNA level of sclerostin (SOST), normalized to house-keeping gene HPRT, and (B) Plasma SOST concentration at the end point (□, ActRIIB.Fc; ▲, saline control). Results were shown as dot plots with each dot represents on individual animal, and analyzed by unpaired *t*-test.

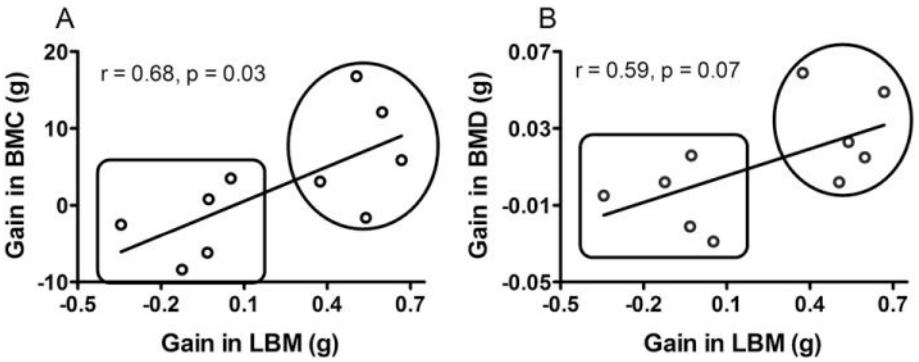

Fig. 5.

Association between the gain in lean body mass (LBM) and bone mineral content (A, BMC) or bone mineral density (B, BMD). Results were shown as dot plots with each dot represents on individual animal, and analyzed by Pearson correlation test. Results in the upper circles belong to the group treated with ActRIIB.Fc, and those in the lower square belong to the saline control group.